Lab on a Chip

Magnetic bead chains for surface enhancement in microfluidic electrochemical biosensor platforms

Journal:	*Lab on a Chip*
Manuscript ID:	LC-ART-07-2015-000796.R1
Article Type:	Paper
Date Submitted by the Author:	15-Aug-2015
Complete List of Authors:	Armbrecht, Lucas; University of Freiburg, Department of Microsystems Engineering - IMTEK Dincer, Can; University of Freiburg, Department of Microsystems Engineering - IMTEK; University of Freiburg, Freiburg Materials Research Center - FMF Kling, Andre; University of Freiburg, Department of Microsystems Engineering - IMTEK Horak, Josef; University of Freiburg, Department of Microsystems Engineering - IMTEK; KTH Stockholm, Division for Chemical Protein Engineering Kieninger, Jochen; University of Freiburg, Department of Microsystems Engineering - IMTEK Urban, Gerald; University of Freiburg, Department of Microsystems Engineering - IMTEK; University of Freiburg, Freiburg Materials Research Center - FMF

Journal Name

ARTICLE

Self-assembled magnetic bead chains for sensitivity enhancement of microfluidic electrochemical biosensor platforms

Received 00th January 20xx,
Accepted 00th January 20xx

DOI: 10.1039/x0xx00000x

www.rsc.org/

L. Armbrecht[a], C. Dincer[a,b], A. Kling[a], J. Horak[a,c], J. Kieninger[a] and G. Urban[a,b]

In this paper, we present a novel approach to enhance the sensitivity of microfluidic biosensor platforms with self-assembled magnetic bead chains. An adjustable, more than 5-fold sensitivity enhancement is achieved by introducing a magnetic field gradient along a microfluidic channel by means of a soft-magnetic lattice with a 350 µm spacing. The alternating magnetic field induces self-assembly of the magnetic beads in chains or clusters and thus improves the perfusion and active contact between analyte and beads. The soft-magnetic lattices can be applied independent of the channel geometry or chip material to any microfluidic biosensing platform. At the same time, the bead-based approach obtains chip-reusability and shortened measurement times. The bead chain properties and the maximum flow velocity for bead retention were validated with optical microscopy in a glass capillary. The magnetic actuation system was sucessfully validated with a biotin-streptavidin model assay on a low-cost electrochemical microfluidic chip, fabricated in dry-film photoresist technology (DFR). Labelling with glucose oxidase (GOx) permitts rapid electrochemical detection of enzymatically produced H_2O_2 .

Introduction

Since the 1990s, microfluidic biosensor systems utilizing solid micro-particles (beads) became popular.[1,2] Microfluidic systems benefit from small dimensions and reaction volumes, thus enhancing the time-to-result and lowering the analyte volume at high sensitivities.[3,4] Besides polyimide, silica or agar-based beads, super-paramagnetic particles composed of magnetic nanoparticles, embedded in a polymeric matrix have become a common analytical tool in biological labs.[5] Microfluidic biosensor systems largely benefit from these spherical magnetic microparticles.[6,7] The possibility of magnetic manipulation, combined with their high surface-to-volume ratio enables fabrication of re-usable, highly sensitive on-chip biosensors for various applications.[8,9] Additionally, magnetic bead actuation is utilized for biosensing as well as cell separation in platforms that use droplet microfluidic approaches.[10]

In the last 15 years, significant progress in the manipulation of magnetic beads on-chip has been achieved.[11] In order to realize highly sensitive bead-based microfluidic biosensors, the active contact between beads and sample has to be maximized. Here, high perfusion of the sample allows the capture of a maximum number of target molecules, which leads to enhanced signals.[12-16] Bead-based immunoassay platforms with varying channel cross-sections in combination with permanent magnets have been presented.[17] Integrated electromagnets and highly complex dynamic systems linking external electromagnets and permanent magnets have also been proposed.[18,19] The active manipulation of magnetic beads inside microfluidic channels offers new chances for the performance of a large variety of reliable, sensitive and low cost biological tests. Nevertheless, the complexity of the manipulation system and/or the requirements for the chip design of the aforementioned manipulation techniques still prevent from their widespread use.

Enzyme-linked immunosorbent assays (ELISA) are still the most sensitive, specific and selective measurement method for the qualitative and quantitative detection of biomarkers.[20] They have been extensively studied in various disciplines as biology, medicine, food safety monitoring, chemistry and other research fields with detection limits down to the pg ml^{-1} range.[21-24] In this work, we mimic these biological binding assays with a biotin-streptavidin model assay, labelled with glucose oxidase. Detection of biological assays is commonly done via optic absorbance or chemiluminescence measurements.[25,26] In contrast to these techniques, electrochemical detection of enzymatically produced H_2O_2 takes advantage from fast read-out due to the intrinsic enzymatic amplification, independence of the optical chip properties and easy miniaturization of chip and measurement setup. Therefore, electrochemical detection is well suited for point of care (POC) diagnostic systems.[27]

[a.1] Laboratory for Sensors, Department of Microsystems Engineering - IMTEK, University of Freiburg, 79110 Freiburg, Germany.
[b.2] Freiburg Materials Research Center - FMF, University of Freiburg, 79110 Freiburg, Germany
[c.3] Division for Chemical Protein Engineering, KTH Stockholm, Stockholm, Sweden
Electronic Supplementary Information (ESI) available: [details of any supplementary information available should be included here]. See DOI: 10.1039/x0xx00000x

Microfluidic electrochemical biosensors, fabricated in DFR technology, benefit from low production costs and possible mass fabrication on roll-to-roll processes. They have already been proposed by Horak et al. as disposable sensors for the detection of different analytes.[28,29] In this work, the previous DFR based sensor platform is extended to a bead-based sensor platform. It combines DFR technology with a new cost-efficient, small and universally applicable magnetic actuation principle. This is based on a soft-magnetic lattice, fabricated by lamination of soft-magnetic and non-magnetic foils into a stack. Combined with permanent magnets, these structures create a magnetic field gradient along the microfluidic channel in the underlying microfluidic chip. This leads to self-assembly of magnetic beads in chain like structures with improved contact between the beads and the solution. In comparison to other techniques this allows low-cost mass fabrication of the manipulation device without any need for complex machinery. Furthermore, external application enhances the flexibility in chip design.[17-19]

We optically observed the influence of the soft-magnetic lattice application on the bead distribution in the micro-channel as well as the bead retention under flow conditions. Electrochemical validation was performed on the redesigned DFR based biosensor chip, utilizing a custom-made measurement adapter. A more detailed description of the DFR technology and the characterization of the biosensor chip is given in the Electronic Supplementary information (ESI).

Experimental

Fabrication of soft-magnetic lattices

Fig. 1a illustrates the fabrication of soft-magnetic lattices in lamination technique. Mu-metal foil (Vacuumschmelze GmbH & Co. KG, Germany) and double-sided sticky tape (Tesa, Germany) in thicknesses of 100, 350 and 500 µm are laminated to a multilayer stack of 13 mm. Subsequent embedment in a polymeric matrix ensures mechanical stability and a final grinding step releases the soft-magnetic lattice structure. . The investigated lattice spacings are a tradeoff between high magnetic field gradients for bead capture and small distances between bead chains improving the diffusion of analyte towards the beads. Detailed information thereof is given in the ESI.

In order to compare the lamination approach to existing structuring methods of soft-magnetic materials, an additional lattice in 350 µm spacing was fabricated by electrochemical discharge machining (EDM) out of 100 µm thick Mu-metal foil. The fabricated devices are shown in Fig. 1b.

Actuation of magnetic beads

The magnetic force that acts on an individual magnetic bead is defined by the bead properties and the applied external magnetic field. In the saturation region, the force is given by [30]

$$\vec{F}_{mag} = (\vec{m}_{sat} \cdot \nabla)\vec{B} \quad (1)$$

in which $\vec{m}_{sat}$ is the magnetization of the bead in saturation and $\vec{B}$ the induced magnetic flux density. As seen in eqn. (1), for a given particle magnetization, the magnetic force is directly dependent on the gradient of the magnetic field. The viscous drag is counteracting this force and, assuming fluid flow only in the x-direction, the maximal flow velocity for bead retention is consequently given by [30]

$$v_{x,max} = \frac{m_{sat}}{6 \cdot \pi \cdot \eta \cdot r_{bead}} \cdot \frac{d\vec{B}}{dx} \quad (2)$$

where m_{sat} is the beads saturation magnetization in x-direction, η the dynamic viscosity of the medium, r_{bead} the particles radius and dB/dx the magnetic field gradient in x-direction.

Setup for optical investigations

For real-time monitoring of magnetic beads under flow conditions and optical visualization of bead chains, a setup out of a transparent glass capillary (Hilgenberg GmbH, Germany; I.D.: 80 µm; O.D.: 120 µm), a syringe pump (PHD2000 Harvard Aparatus, USA; syringes from Hamilton Company, USA) and the magnetic actuation as illustrated in Fig. 2a was used. The

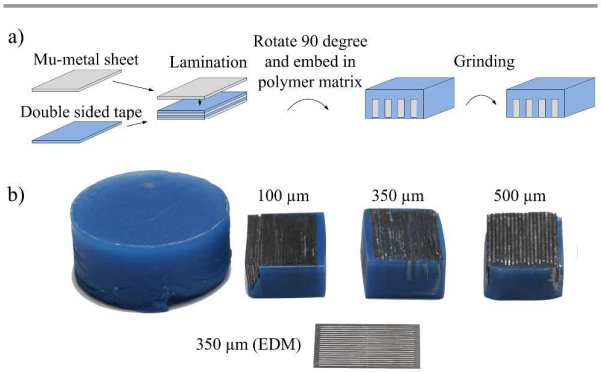

Fig. 1: Soft-magnetic lattices used for the manipulation of magnetic microparticles. (a) Lamination of Mu-metal foils and double-sided adhesive tape is followed by encapsulation in a polymeric matrix and subsequent grinding. (b) Polymeric block and final lattice structures with well-defined lattice spacings fabricated by lamination and EDM.

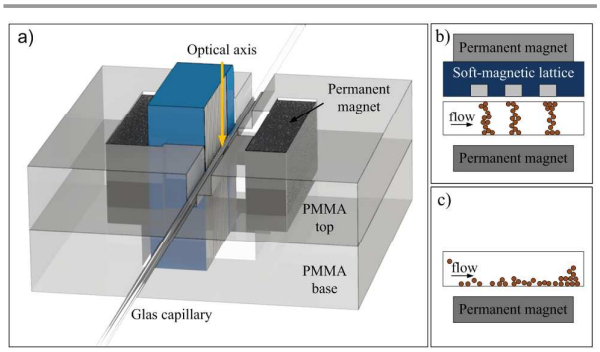

Fig. 2: (a) Schematic view on the optical investigation system for evaluation of the magnetic actuation by soft-magnetic lattices. (b) Principle of the bead chain formation at locations of high magnetic flux density, induced by application of soft-magnetic lattices. (c) In the monopolar setup without lattice structure, the beads accumulate at the channel walls with low perfusion of the medium leading to minor analyte capture rates.

magnetic actuation system was located perpendicular to the glass capillary enabling microscopy from above. To allow easy disassembly of the capillary from the magnetic actuation system, the two 20 x 10 x 4 mm³ sized NdFeB permanent magnets as well as the soft-magnetic structure were fixed on a transparent 4 mm thick PMMA base. The glass capillary that resembles the microfluidic channel was glued onto a second, independent plate (PMMA top).

Before the magnetic parts were attached, 5 µl of solution with the desired concentration of monodisperse 1.43 µm streptavidin coated magnetic beads were introduced into the capillary. The PMMA top was subsequently mounted onto its counterpart for magnetic actuation. Deionized water was withdrawn through the micro-capillary at flow rates of up to 10 mm sec^{-1} with the previously mentioned syringe pump. Pictures of the bead chain formation were taken at different bead concentrations and flow velocities for the 100 µm, 350 µm and 500 µm laminated lattices.

DFR-based biosensor chip fabrication

Pyralux® AP 8525R (DuPont™, USA) in 50 µm thickness is used as the substrate for wafer-level processing of the biosensor chip. Photoresist ma-N 1420 (Micro Resist Technology GmbH, Germany) is spin-coated onto the PI-substrate and structured. A 200 nm platinum layer was then evaporated onto the substrate under cleanroom conditions. Metal patterns were released in a subsequent lift-off-process.

The next steps were spin coating and lithographic structuring of a 5 µm thick SU-8 3005 (MicroChem Corp. USA) isolation layer, defining the electrode sizes and an additional well for the stop barrier. The microfluidic channels were subsequently realized with the DFR material Pyralux® PC1025 (DuPont™, USA) in a thickness of 64 µm. Then the Ag/AgCl reference electrode is fabricated by electrodeposition of silver, followed by a chloridation step. The physical barrier is realized by dispensing a small drop of 1% Teflon (DuPont™, USA) solution into the predefined wells in the SU-8 isolation layer of the chip. After evaporation of the solvent a thin Teflon layer is formed, that is sufficient to act as a flow barrier during capillary filling. Finally, the cover-layer with the fluidic inlet and outlet ports are realized in an additional DFR layer. To prevent from bending effects due to thermal expansion effects during baking, symmetry was achieved by laminating two layers of DFR on the backside of the wafer. The chips are thereafter cut into duplicates and backed in the oven for 3 hours at 160 °C. The resulting flexible biosensor chips (Fig. 3a) have a size of 25.65 x 10.20 mm². The working electrodes size is 0.311 mm², the channel width 500 µm and the microfluidic channel up to the stop barrier, the bead capture region, holds approximately 3.2 µl of analyte.

A comparable processing based on a different DFR material has already been shown by Horak et al.[24]

Magnetic, electrochemical and microfluidic setup

The sensor is mounted on a custom-made adapter prior to measurements. Fig. 3b presents this measurement adapter for electric and fluidic connection to the periphery as well as magnetic actuation. Fast and reliable electrical connection to a four channel bi-potentiostat (Jobst technologies GmbH, Germany) is realized. The setup enables facile chip connection and parallel measurement of up to four biosensor chips. The fluidic connection is established by screwing a PMMA-connector onto the PMMA base. In contrast to pressure seals, the employed 0.125 " vacuum cups (Nordson EFD, Germany) are more flexible and allow tight sealing without the risk of channel compression or pinch off.

Electrochemical measurements on-chip

As illustrated in Fig. 3c, the the measurement cell consists of a Ag/AgCl reference electrode and two Pt electrodes used as working and counter electrode in amperometric measurements. The working electrode detects enzymatically produced H_2O_2 at 450 mV vs. Ag/AgCl. Glucose oxidase, producing H_2O_2 from a glucose solution, was used as an enzymatic label. All solutions were prepared in ultra-pure, HPLC grade water (Alpha Aeser, USA).

After introduction of the beads, 100 mM phosphate buffered saline (PBS), 137 mM NaCl, 2.7 mM KCl, 10 mM Na_2HPO4, 2 mM KH_2PO_4, at pH = 7.4 was withdrawn through the microfluidic channel at a mean flow velocity of 1.5 mm sec^{-1} (flow rate of 2.88 µl min^{-1}). When the amperometric signal

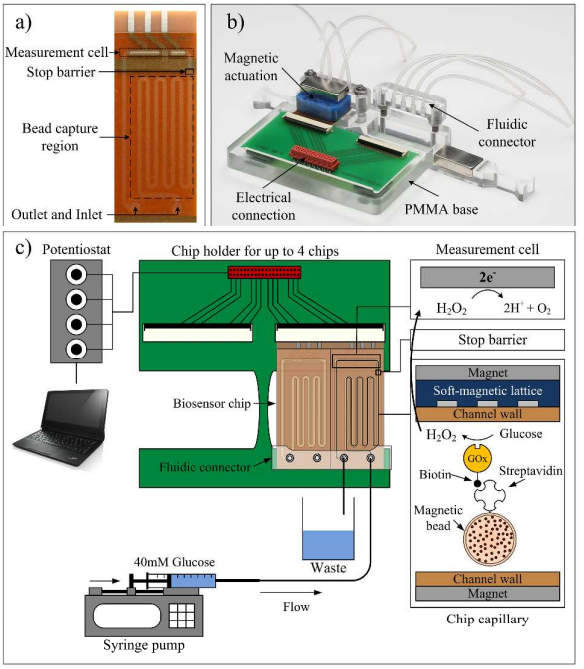

Fig. 3:(a) On-chip measurements are performed on an electrochemical DFR-based biosensor platform. It benefits from flexibility as well as from low-costs and allows for mass fabrication. (b) Up to four chips can be analysed in parallel on the custom-made measurement adapter. The PCB preserves a fourth electric connection that is not used here. (c) Electrical read-out with a four-channel bi-potentiostat detects enzymatically produced H_2O_2, produced from the 40 mM glucose substrate supplied by a standard syringe pump. Biotinylated GOx is bound to the streptavidin-coated bead surface while the beads are actuated with the previously described magnetic system.

reached a stable steady-state current (baseline), the 40 mM glucose substrate, diluted in 100 mM PBS (pH = 7.4), was introduced and stop-flow measurements were performed. In the stop phase, H_2O_2 accumulates in the channel and is subsequently flushed over the working electrode when the flow is restarted. The generated current peak is visualized with the software BioMON (Jobst technologies GmbH, Germany) on a computer.[31]

Biotinylated GOx model assay

Streptavidin-coated magnetic beads (Microparticles GmbH, Germany) with a diameter of 1.43 µm were used for all experiments. The biotinylated GOx (bGOx) model assay takes advantage of the strong affinity of biotin to streptavidin.[29] When getting in close proximity, bGOx binds to the streptavidin-coated magnetic beads. Dilution of the magnetic beads was done by diluting the stock solution (10 mg ml^{-1} bead-content) 10-fold and 100-fold in 0.1 M PBS.

To experimentally validate the functionality of the fabricated soft-magnetic lattice structures, the appropriate bead dilution was washed with 10 mM phys. PBS (pH = 7.4) and incubated for 30 min with up to 1 µg ml^{-1} bGOx. After subsequent washing with wash buffer (phys. PBS with 1% Tween 20) on a magnetic holder (Dynal technologies, Norway), 3.5 µl of the solution were introduced to the biosensors by capillary filling and the chips were mounted onto the measurement adapter.

To prevent from unspecific adsorption during on-chip immobilization-tests, the chips were blocked for 1 h with 1% bovine serum albumin (BSA) in phys. PBS and washed with 200 µl of wash buffer. Then, the 0.1 mg ml^{-1} bead dilution was introduced to the micro-capillary with the syringe pump, incubated with 200 ng ml^{-1} bGOx on-chip and washed by withdrawal of 20 µl wash buffer previously to measurements.

Results and discussion

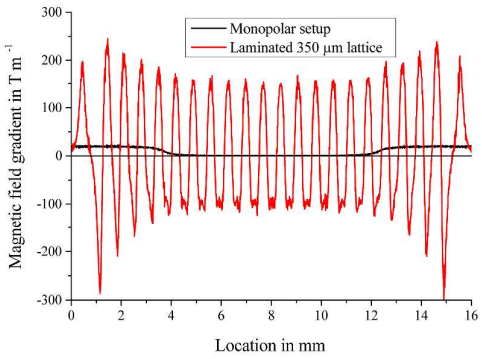

Fig. 4: Influences of soft-magnetic lattice application on the magnetic flux profile in a distance of 100 µm was simulated using the open source program FEM. A lattice with 350 µm spacings (red) results in an alternating magnetic field compared to a monopolar setup without lattice structure (black). With the help of eqn. 2, a maximum flow for bead retention of 3.44 mm sec^{-1} is estimated.

Simulation

Simulation of the magnetic flux inside the microfluidic channel was done with the open source program FEMM (D. C. Meeker, Finite Element Method Magnetics, Version 4.0.1) in a distance of 100 µm from the soft-magnetic lattice. This value represents the distance between the DFR cover layer and the center of the microfluidic channel in the biosensor chip. Employing 10 x 20 x 4 mm^3 permanent neodymium-iron-boron (NeFeB) magnets (Webcraft GmbH, Germany) and a 350 µm spaced laminated soft-magnetic lattice, the 2-D FEM simulations show formation of a magnetic field gradient in the microfluidic channel (Fig. 4). The utilized setup consisted of a permanent magnet underneath the biosensor chip and the lattice structure as well as a second permanent magnet applied to the channel cover. According to eqn. 2, capture of 1.43 µm sized magnetic beads (Microparticles GmbH, Germany) takes place at the local maxima of the magnetic flux gradient. Hence, the shown combination of lattice and magnets retents the 1.43 µm sized magnetic beads up to a flow velocity of 3.44 mm sec^{-1}.

Lamination of soft-magnetic lattices

The fabrication of soft-magnetic lattices by lamination proved to be fast and facile. Lattice spacing down to 100 µm were fabricated without any noticeable issues. The advantages of this technology are low costs, high structure thicknesses, fast processing and huge flexibility in design compared to other suitable techniques like EDM, etching, puls-lasering, etc. Additionally, no external equipment is necessary during fabrication and no heat is introduced.

Structures and properties of the bead formation

Fig. 5a shows, that application of the soft-magnetic lattices results in the formation of magnetic bead clusters. These consist of multiple bead chains with the distance between individual clusters being defined by the lattice spacing. The bead structures tend to accumulate at the top of the channel due to the enlarged distance to the permanent magnet on this side of the micro-capillary in the optical setup. However, this effect is averted on the electrochemical measurement adapter since the magnetic parts are directly applied to the channel resulting in a highly symmetric setup.

Figure 5b, c and d represent the self-assembled bead-structures at bead concentrations of 1 mg ml^{-1}, 0.1 mg ml^{-1} and 0.01 mg ml^{-1}. The higher the bead concentration, the larger the bead clusters and the better is the channel perfusion.

The resistance of these bead structures against fluid flow was investigated using a 350 µm laminated lattice. Deionized water as substrate was supplied and the mean flow velocity was increased stepwise.

On-line visualization enabled determination of the maximum flow velocity for bead retention. Fig. 5e and f show that bead chains withstand flow velocities up to 3 mm sec^{-1} and cover a significantly higher fraction of the channel cross-section than in the monopolar setup (Fig. 5g). Furthermore, these optical results match with the analytical estimations based on the

magnetic simulations, yielding a theoretical maximum flow velocity of 3.44 mm sec^{-1}.

Characterization of the electrochemical biosensor platform

Wafer-level fabrication of the DFR biosensor chips was followed by their characterization. A detailed description is given in the ESI.

It was found that the biosensor chips have a linear and reproducible H_2O_2-sensitivity of 6 nA mm^{-2} μM^{-1} at a flow velocity of 1.5 mm sec^{-1}. Washing with wash buffer verified the ability to remove almost all beads from the microfluidic channel. Therefore, re-usability of the chips is also possible. Stop flow measurements produce a detectable signal peak resulting from the accumulation of enzymatically produced H_2O_2 in the microfluidic channel. It was proven, that the peak charge and peak current in stop-flow measurements are proportional. Thus, the peak current can be taken as the measurement signal.

Electrochemical measurements with pre-immobilized beads

After characterizing the sensor platform, evaluation of the magnetic actuation with soft-magnetic lattices had to be done. Electrochemical measurements were performed with beads that were pre-immobilized with different bGOx concentrations in standard lab tubes. Fig. 6 shows the results of the measured continuous flow signal (baseline), the 2 min. and the 5 min. stop-flow peak current densities after introduction of 3.5 µl of bead solution into the microfluidic capillary and subsequent magnetic actuation. The different magnetic actuation setups were experimentally tested with a bead-concentration of 0.1 mg ml^{-1}. A significant increase in the signal was seen, when soft-magnetic lattices were applied. Lamination was found to be the superior technology for lattice fabrication compared to EDM, even though EDM preserves higher surface qualities. The reason is the enormous lattice thickness of the laminated devices (several mm) that cannot be achieved by EDM or other high precision fabrication techniques.

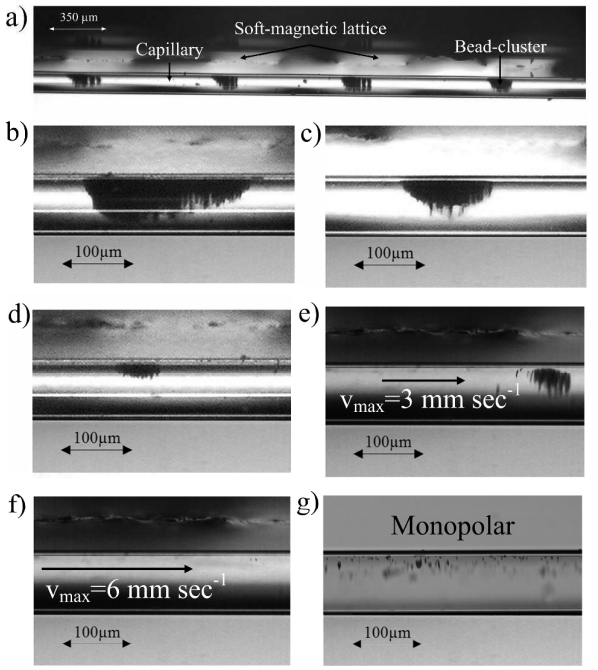

Fig. 5: Optical visualization of the bead chain formation. Bead clusters arrange at locations of close proximity to the Mu-metal lattice. Larger lattice spacings result in formation of bead clusters instead of single chains, but are able to penetrate the chip cover and evoke high magnetic forces. (a): The distance between clusters is defined by the lattice spacing (350 µm lattice shown in this picture). (b), (c) and (d): Different bead concentrations (from left to right: 1 mg ml^{-1}, 0.1 mg ml^{-1} and 0.01 mg ml^{-1}) induce different sizes of the bead plugs and channel perfusion. As seen in (e) and (f), beads withstand flow rates up to 3 mm sec^{-1}. (g): The monopolar setup with 1 mg ml^{-1} beads with significantly lower bead capture and no visible bead chain formation.

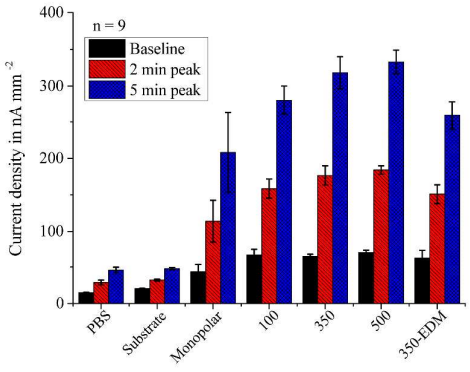

Fig. 6: Electrochemical measurements for different magnetic setups. Streptavidin coated magnetic beads were incubated with 1 µg ml^{-1} bGOx for 30 min off-chip and then introduced to the biosensor-chip. 350 µm and 500 µm lattice spacings show a 1.7-fold increase in the sensitivity compared to the monopolar setup. Due to the small thickness of the EDM-cut lattice, the low-cost laminated lattices show a better performance.

The 100 µm lattice spacing showed significantly less signal compared to the 350 µm and 500 µm spacings. This is related to the distance between beads and soft-magnetic lattice, which is in the same size as the lattice spacing. This leads to a decrease in the amplitude of the magnetic field gradient in the microfluidic channel. Hence, bead capture and bead-chain formation cannot be guaranteed. Different concentrations of bGOx were subsequently applied to investigate the effect of the lattice-application over a concentration range from 0.32 ng ml^{-1} to 1 µg ml^{-1} of bGOx during incubation with magnetic beads in lab tubes.

Fig. 7a shows the 5 min. stop-flow peak current densities of the aforementioned measurements. It was seen, that the 350 and 500 µm laminated soft-magnetic lattices were able to enhance the electrochemical signal of pre-immobilized beads by a factor of 1.7 at a three times lower standard deviation. This is explained by the formation of magnetic bead chains and clusters leading to a more homogeneous bead distribution in the channel and improved contact between beads and solution. This effect was seen over the whole concentration range and for two different bead concentrations of 1 and 0.1 mg ml^{-1}. Besides, it was found that the sensitivity of the platform could be tuned by increasing the introduced bead amount. Nevertheless, an increased bead concentration

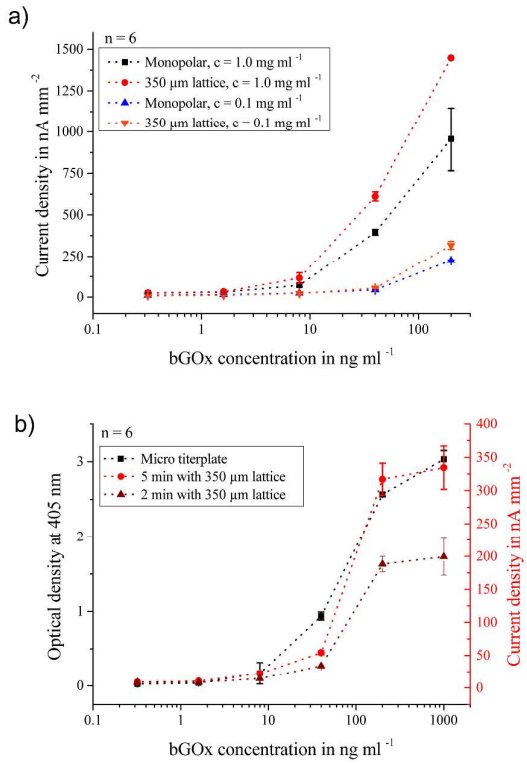

Fig. 7: Biotin-GOx model assay performed on streptavidin-coated magnetic beads. The beads were incubated with bGOx off-chip and then introduced prior to measurement. (a) Application of lattice structures in 350 µm spacing as well as enhancing the bead concentration improves the sensitivity of the DFR biosensor platform. (b) The electrochemical biosensor platform with magnetic beads shows the same detection limit as the micro-titer plate format for the given test-assay on beads.

without allocation of a lattice structure also leads to higher measurement errors. This can be explained by the accumulation of beads at the end of the permanent magnet in the monopolar setup. The limited space at this location results in a loss of beads that are forced in larger distances to the magnet and can thus no longer withstand the flow.

Microtiter-plates are a commonly used and well established technique for the detection of biological assays. Therefore, pre-immobilized beads were measured on microtiter-plate format and on the magnetic bead-based electrochemical biosensor platform. In contrast to the chip platform, the microtiter-plate format is limited to bead concentrations of up to 0.1 mg ml^{-1} due to the optical properties of the beads caused by their high iron oxide content. For comparability, all tests shown in Fig. 7b were done with a bead concentration of 0.1 mg ml^{-1}. It was seen, that our platform shows the same signal characteristics as the microtiter-plate format. On both formats, the limit of detection (LOD) was 8 ng ml^{-1}. Additionally, the measurement duration on-chip was reduced to 2 min on the electrochemical biosensor system. Furthermore, only 3.5 µl of bead solution and analyte volume are necessary, compared to 100 µl used on the microtiter-plate format.

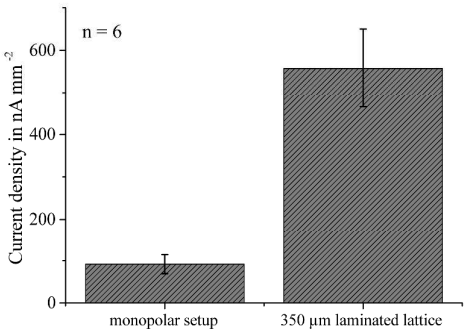

Fig. 8: Biotin-GOx model assay performed on streptavidin-coated magnetic beads on-chip. Beads were incubated with 200 ng ml^{-1} bGOx for 15 min in the microfluidic channel. The resulting enhancement of the platforms sensitivity compared to a monopolar setup is more than 5-fold, when soft-magnetic lattices are applied to the biosensor chip.

Electrochemical measurements with on-chip immobilization

To prove the efficiency of the increased active contact between beads and analyte under the application of soft-magnetic lattices, on-chip immobilization of beads was performed. Therefore, 10 µl of the streptavidin-coated magnetic beads were introduced into the microfluidic channel of the biosensor chip with the syringe pump. Then, the magnetic actuation system was applied and 10 µl of analyte were withdrawn through the channel at a mean flow velocity of 1.5 mm sec^{-1}. When the analyte was located at the immobilization area, flow was stopped for a 15 min incubation step. After 5 min washing with 0.1 M PBS, the 40 mM glucose substrate was supplied at a mean flow velocity of 1.5 mm sec^{-1} and electrochemical stop-flow measurements were conducted.

Fig. 8 compares the generated signals for a bGOx concentration of 200 ng ml^{-1} incubated with and without application of the soft-magnetic lattice. It was seen, that the increase in platform sensitivity evoked by lattice-application is higher than the 1.7-fold increase in case of pre-immobilized beads. The reason is the improved analyte capture in the channel due to the bead chain formation, which cannot be investigated with pre-immobilized beads. A more than 5-fold amplification was achieved with the 350 µm laminated soft-magnetic lattice compared to the monopolar setup.

Conclusion

In this work, we presented a magnetic bead-based biosensor platform, which combines DFR technology together with soft-magnetic lattices. The soft-magnetic lattices are produced by lamination of soft-magnetic and non-magnetic foils. Lamination as fabrication technique for soft-magnetic lattices benefits from low costs and allows the realization of lattice thicknesses in the mm- to cm-range. Nevertheless, the lower limit in the lattice spacing is defined by the distance between beads and lattice structure (chip cover). Optical investigation of the self-alignment of magnetic beads in chains and clusters

revealed possible bead retention up to flow velocities of 3 mm sec^{-1} in deionized water. Furthermore, it was verified that the distance in between and the size of bead structures is tunable by the amount of introduced beads and the spacing of the soft-magnetic lattice.

Compared to the monopolar setup, the application of laminated soft-magnetic lattices with a 350 µm lattice spacing shows a more than 5-fold increase in the current signal for on-chip immobilization tests using a bGOx model assay on magnetic beads. Even for pre-immobilized beads, the formation of magnetic bead chains and clusters resulted in an almost 2-fold signal enhancement over the whole measured concentration range of bGOx.

Laminated soft-magnetic lattices as a magnetic actuation method can be applied to a huge variaty of magnetic bead-based microfluidic biosensor platform and represent a cheap and facile solution to significantly increase the sensitivity of such platforms.

Acknowledgements

The authors would like to thank Prof. Thomas Hanemann from the Laboratory for Materials Processing of the Department of Microsystems Engineering - IMTEK, University of Freiburg for his support.

References

1 A. Manz, N. Graber and H. M. Widmer, *Sens Actuators B Chem*, 1990, **1**, 244-248.
2 M. A. M. Gijs, *Microfluidics and Nanofluidics*, 2004, **1**, 22-40.
3 E. Verpoorte, *Lab Chip*, 2003, **3**, 60N-68N.
4 T. M. Phillips and E. F. Wellner, Electrophoresis, 2007, **28**, 3041-3048.
5 D. Raps, N Hossieny, C. B. Park and V. Altstädt, *Polymer*, 2014, **56**, 5-19.
6 E. Paleček and Miroslav Fojta, *Talanta*, 2007, **74**, 276-290.
7 O Phillippova, A. Barabanova, V. Molchanov and A. Khokhlov, *Eur. Polym. J.*, 2011, **47**, 542-559.
8 J. A. Thompson and H. H. Bau, *J. Chromatogr. B*, 2010, **878**, 228-236.
9 A. RIda and M. A. M. Gijs, *Anal. Chem.*, 2004, **76**, 6239-6246.
10 H. Lee, L. Xu, and K. W. Oh, Biomicrofluidics, 2014, **8**(4), 044113.
11 N. Pamme, *Lab Chip*, 2006. **6**, 24-38.
12 S. V. Kergaravat, G. A. Gómez, S.N Fabiano, T. I. L. Chávez, M. I. Pividori and S. R. Hernández, *Talanta*, 2012, **97**, 484-490.
13 S. A. Peyman, A. Iles and N. Pamme, *Lab Chip*, 2009, **9**, 3110-3117.
14 N. Pamme, J. C. Eijkel and A. Manz, *J. Magn. Magn. Mater.*, 2006, **302**, 237-244.
15 W. C. Lee, K. Y.Lien, G. B. Lee and H. Y. Lei, *Diagn. Microbiol. Infect. Dis*., 2008, **60**, 51-58.
16 M. Bu, T. B. Christensen, K. Smistrup, A. Wolff and M. F Hansen, *Sensors Actuators A Phys.*, 2008, **145-146**, 430-436.
17 F. Lacharme., C. Vandevyver and M. A. M. Gijs, *Anal. Chem.*, 2008, **80**, 2905-2910.
18 J. W. Choi, C. H. Ahn, S. Bhansali and H. T. Henderson. *Sensors Actuators B Chem.*, 2000, **68**, 34-39.
19 Y. Moser, T. Lehnert and M. A. M. Gijs, *Lab Chip*, 2009, **9**, 3261-3267.
20 R. Mazurczyk, J. Vieillard, A. Bouchard, B. Hannes and S. Krawczyk, *Sensors Actuators B Chem.*, 2006, **118**, 11–19.
21 J. W. A. Findlay, W. C. Smith, J. W. Lee, G. D. Nordblom, I. Das, B. S. DeSilva, M. N. Khan and R. R. Bowsher, *J. Pharm. Biomed. Anal.*, 2000, **21**, 1249–1273.
22 P. B. Luppa, L. J. Sokoll and D. W. Chan, Clin. Chim. Acta, 2001, 314, 1–26.
23 M. Hervás, M. A. López and A. Escarpa, *Analyst*, 2011, **136**, 2131–2138.
24 A. Escarpa, *Lab Chip*, 2014, **14**, 3213.
25 B. Otieno, C. E. Krause, A. Latus, B. V Chikkaveeraiah, R. C. Faria and J. F. Rusling, *Biosens. Bioelectron.*, 2014, **53C**, 268–274.
26 M. Iranifam, *TrAC Trends Anal. Chem.*, 2013, **51**, 51–70.
27 Z. Herrasti, I. Etxabe, J. M. Mitxelena, I. Gabilondo, M. P. Martínez and F. Martínez, *Sensors Actuators B Chem*., 2013, **189**, 66–70.
28 J. Horak, C. Dincer, H. Bakirci and G. Urban, *Sensors Actuators B Chem.*, 2014, **191**, 813–820.
29 J. Horak, C. Dincer, E. Qelibari, H. Bakirci and G. Urban, *Sensors Actuators B Chem.*, 2015, **209**, 478–485.
30 S. S. Shevkoplyas, A. C. Siegel, R. M. Westervelt, M. G. Prentissc and G. M. Whitesides, *Lab Chip*, 2007, 1294–1302.
31 A. Weltin, K. Slotwinsk, J. Kieninger, I. Moser, G. Jobst, M. Wego, R. Ehret, G.A. Urban, *Lab Chip*, 2014, **14**, 138-146.
32 P. Weber, D. Ohlendorf, J. Wendoloski and F. Salemme, *Science*, 1989, **243**, 85–88.